A Single Amino Acid Change in Rabies Virus Glycoprotein Increases Virus Spread and Enhances Virus Pathogenicity

Milosz Faber,[1] Marie-Luise Faber,[2] Amy Papaneri,[1] Michael Bette,[3] Eberhard Weihe,[3] Bernhard Dietzschold,[1] and Matthias J. Schnell[1]*

Department of Microbiology and Immunology, Thomas Jefferson University, Philadelphia, Pennsylvania 19107[1];
Molecular Targeting Technologies, 882 S. Matlack St., Suite 105, West Chester, Pennsylvania 19382[2];
and Department of Molecular Neuroscience, Institute of Anatomy and Cell Biology,
Philipps University Marburg, Marburg, Germany[3]

Several rabies virus (RV) vaccine strains containing an aspartic acid (Asp) or glutamic acid (Glu) instead of an arginine (Arg) at position 333 of the RV glycoprotein (G) are apathogenic for immunocompetent mice even after intracranial inoculation. However, we previously showed that the nonpathogenic phenotype of the highly attenuated RV strain SPBNGA, which contains a Glu at position 333 of G, is unstable when this virus is passaged in newborn mice. While the Glu_{333} remained unchanged after five mouse passages, an $Asn_{194} \rightarrow Lys_{194}$ mutation occurred in RV G. This mutation was associated with increased pathogenicity for adult mice. Using site-directed mutagenesis to exchange Asn_{194} with Lys_{194} in the G protein of SPBNGA, resulting in SPBNGA-K, we show here that this mutation is solely responsible for the increase in pathogenicity and that the $Asn_{194} \rightarrow Lys_{194}$ mutation does not arise when Asn_{194} is exchanged with Ser_{194} (SPBNGA-S). Our data presented indicate that the increased pathogenicity of SPBNGA-K is due to increased viral spread in vivo and in vitro, faster internalization of the pathogenic virus into cells, and a shift in the pH threshold for membrane fusion. These results are consistent with the notion that the RV G protein is a major contributor to RV pathogenesis and that the more pathogenic RVs escape the host responses by a faster spread than that of less pathogenic RVs.

Rabies is a major zoonotic disease that remains an important public health problem, causing 60,000 annual deaths worldwide (15). In the Americas, rabies virus (RV) circulates in many wild animal species, which represent the major rabies reservoirs (23). Oral immunization of wildlife with live attenuated RVs or recombinant RV vaccines is the most effective method to control and eventually eradicate rabies (1, 29). For live attenuated RV vaccines, safety is the foremost criterion. According to World Health Organization recommendations, any live RV that can be used for immunization of wildlife must not cause disease in immunocompetent mice following intracerebral (i.c.) infection.

The RV glycoprotein (G) is a major contributor to the pathogenicity of the virus (6, 16, 20, 26). Several G-associated pathogenic mechanisms have been identified: (i) G must interact effectively with cell surface molecules that can mediate rapid virus uptake (5, 9, 13); (ii) G must interact optimally with the RNA-NP-M complex for efficient virus budding (18); and (iii) expression levels of G must be controlled to prevent functional impairment of the infected neuron (20). We demonstrated that the pathogenicity of fixed rabies virus strains (i.e., ERA, HEP, and CVS) correlates with the presence of a determinant located in antigenic site 3 of the G protein (6, 26). We and others showed that virus variants with an Arg→Glu mutation at position 333 affecting antigenic site 3 of the G protein completely lost their ability to kill adult immunocompetent mice, regardless of the site of infection or the virus dose used (6, 16, 17). However, amino acid 333 of G is not the only residue that determines the pathogenic phenotype of an RV. Ito et al. (12), who compared the G protein of the pathogenic Nishigahara strain with that of the nonpathogenic RC-HL strain in a chimeric construct of the two strains, concluded that the amino acid(s) determining the nonpathogenic phenotype of RC-HL must reside between amino acid residues 164 and 303 (12).

A potential problem associated with the use of live attenuated RVs for wildlife immunization rests in the high mutation rate characteristic of RNA viruses. Recently, we constructed three recombinant RVs to carry the G gene of SAD B19 in which Arg_{333} is replaced by a Glu residue. The Glu_{333} G protein, referred to as GA, rendered these viruses nonpathogenic for adult mice after i.c. infection. However, after passaging of these viruses in newborn mice, a single mutation was observed in the G gene of all three recombinant RVs in codons 637 to 639 from AAT (Asn_{194}) to AAG or AAA (Lys_{194}), which was associated with increased pathogenicity. No exchanges in the GAG codon for Glu_{333} were detected in the G genes of the three different RVs after the passages in newborn mice, suggesting that the $Asn_{194} \rightarrow Lys_{194}$ mutation accounted for the reemergence of a pathogenic phenotype. Here we show that the $Asn_{194} \rightarrow Lys_{194}$ mutation in RV G is solely responsible for the reemergence of the pathogenic phenotype, and we delineate the mechanism by which this mutation increases RV pathogenicity.

MATERIALS AND METHODS

Viruses and cell lines. The recombinant RV vector SPBNGA was generated from a SAD B19 cDNA clone as described previously (7, 16). Neuroblastoma (NA) cells of A/J mouse origin were grown at 37°C in RPMI 1640 supplemented with 10% fetal bovine serum (FBS). Cells of another neuroblastoma cell line, N2A, were grown at 37°C in Dulbecco's modified Eagle medium (DMEM)

---

* Corresponding author. Mailing address: 233 South 10th Street, Suite 350 BLSB, Philadelphia, PA 19107-5541. Phone: (215) 503-4634. Fax: (215) 503-5393. E-mail: matthias.schnell@jefferson.edu.

supplemented with 10% FBS. BSR cells (a BHK-21 clone) were grown at 37°C in DMEM supplemented with 10% FBS.

Mice. Six- to 8-week-old female Swiss-Webster mice or pregnant Swiss–Webster mice were purchased from Taconic Farms (Germantown, NY).

Site-directed mutagenesis of RV G and construction of recombinant virus cDNA clones. The RV GA gene was amplified by PCR from full-length pSPBNGA using high-fidelity Deep Vent DNA polymerase (New England Biolabs, Inc., Beverly, MA) and the G gene-specific primers GAM1 (5′-ACG GAA TTC CCC GGG AAG ATG GTT CCT CAG GCT CTC CTG TTT GTA-3′ [EcoRI site underlined; XmaI site in italic; start codon in boldface]) and GAM2 (5′-ACG CTC TAG AGC CCT TAA TTA ACG TTT ACA GTC TGG TCT CAC CCC CA-3′ [XbaI site underlined; PacI site in italic; stop codon in boldface]). The PCR product was digested with EcoRI and XbaI and ligated into pBluescript II SK(+) previously digested with EcoRI and XbaI, resulting in pBGA. The presence of the RV GA gene and the flanking sequences was confirmed by sequencing.

Site-directed mutagenesis was performed using the QuickChange XL site-directed mutagenesis kit (Stratagene, La Jolla, CA) according to the manufacturer's instructions, and primers were designed using Stratagene online software. Primers for lysine were the following: N213K-2(+) (5′-GTC TTG TGA CAT TTT TAC CAA GAG TAG AGG GAA GAG AGC-3′ [lysine codon in boldface]) and N213K-2(−) (5′-GCT CTC TTC CCT CTA CTC TTG GTA AAA ATG TCA CAA GAC-3′ [lysine codon in boldface]); for serine, N213S-4(+) (5′-GAT GTC TTG TGA CAT TTT TAC CTC CAG TAG AGG GAA GAG AGC ATC-3′ [serine codon in boldface]) and N213S-4(−) (5′-GAT GCT CTC TTC CCT CTA CTG GAG GTA AAA ATG TCA CAA GAC ATC-3′ [serine codon in boldface]). Sequences of the modified RV GA genes were confirmed by restriction enzyme analysis and DNA sequencing. The resulting plasmids, designated pBGA-K and pBGA-S for lysine and serine amino acid exchange, respectively, were digested with XmaI and PacI and ligated into pSPBNGA previously digested with XmaI and PacI. The final products were designated pSPBNGA-K and pSPBNGA-S, and the sequences of G genes were verified by sequencing.

Virus rescue from cDNA clones. Recombinant RVs were rescued as described previously (7). Briefly, BSR-T7 cells were transfected using a calcium phosphate transfection kit (Stratagene) with 5.0 μg of SPBNGA-K or SPBNGA-S and 5.0 μg of pTIT-N, 2.5 μg of pTIT-P, 2.5 μg of pTIT-L, and 2.0 μg of pTIT-G. After a 3-day incubation, supernatants were transferred onto BSR cells, and incubation continued for 3 days at 37°C. Cells were examined for the presence of rescued virus by immunostaining with fluorescein isothiocyanate (FITC)-labeled anti-rabies virus N protein antibody (Centocor, Inc., Malvern, PA). The correct nucleotide sequences of the inserted genes were confirmed by reverse transcriptase PCR (RT-PCR) analysis and DNA sequencing.

Preparation of virus stocks and virus titration. BSR cells were infected at a multiplicity of infection (MOI) of 0.1 and incubated for 72 h at 34°C. To determine virus yields, monolayers of NA cells in 96-well plates were infected with serial 10-fold virus dilutions as described previously (9). At 48 h postinfection (p.i.), cells were fixed in 80% acetone and stained with FITC-labeled rabies virus N protein-specific antibody (Centocor, Inc). Foci were counted using a fluorescence microscope, and virus titers calculated in focus-forming units (FFU). All titrations were determined in triplicate.

RNA isolation, RT-PCR, and nucleotide sequence analysis. BSR cells grown in T25 tissue culture flasks were washed with phosphate-buffered saline (PBS), and RNA was extracted using the RNeasy mini-kit (QIAGEN, Valencia, CA) according to the manufacturer's protocol. To isolate RNA from mouse brain tissue, brains were removed, snap-frozen, and homogenized in TRI reagent (Sigma, St. Louis, MO) at a ratio of 1:10; after addition of 200 μl of chloroform to 1 ml of homogenate, samples were incubated at room temperature for 10 min and then centrifuged for 15 min at 12,000 rpm at 4°C, the aqueous phase was collected, and RNA was isolated using the RNeasy mini-kit as described above.

RV G cDNA was synthesized using Superscript One-Step RT-PCR (Invitrogen, Carlsbad, CA) and primers SADB19 −120seq(+) (AACATGTTATGG TGCCATTAAACCGCT) and SADB19 +50seq(−) (GGG TGT TAG TTT TTT TCA TGG ACT TGG). PCR-amplified products were subjected to nucleotide sequencing, and the complete nucleotide sequences of the G genes (including flanking sequences) were obtained and analyzed for the presence of mutations.

Single- and multistep growth curves. Confluent NA cell monolayers grown in T25 culture flasks were infected with RV at a MOI of 5 or 0.01. After incubation for 1 h at 37°C, inocula were removed and cells were washed three times with PBS, cells were replenished with 6 ml of RPMI medium 1640 containing 0.2% bovine serum albumin (BSA) and incubated at 34°C. After infection, 100 μl of

tissue culture supernatant was removed at the indicated time points, and virus was titrated in quadruplicate on NA cells.

Virus spread assay. Virus spread was determined using N2A cells on 60-mm tissue culture plates. Cells cultured for 24 h were washed with PBS, infected with RV at a MOI of 0.01, and incubated for 2 h at 37°C. The inoculum was removed, and cells were washed with PBS. A medium-1% agar mix (equal volumes of 2% agar and 2× DMEM-5% FBS, maintained at 35 to 37°C) was added to each plate and allowed to solidify for 10 min at room temperature. Plates were then incubated at 34°C, and agar was removed at various time points. Cells were washed with PBS, fixed in 80% acetone, and stained with fluorescein isothiocyanate (FITC)-labeled rabies virus N protein-specific antibody (Centocor, Inc.). Thirty fluorescent foci in each plate were analyzed using a fluorescence microscope to determine the average number of infected cells per fluorescent focus.

Kinetics of virus internalization. Kinetics of RV uptake was analyzed as described previously (5). Briefly, monolayers of NA cells grown in 96-well plates were infected with RV at a MOI of 5 and incubated for various times, and noninternalized virus was neutralized by the addition of 2 IU/ml of rabbit polyclonal antirabies serum. At 24 h p.i., the cells were fixed with 80% acetone, stained with FITC-labeled antirabies antibody, and assessed for percentage of rabies antigen-positive cells.

Low-pH-dependent cell fusion. BSR cells were infected with RV at a MOI of 0.5 and incubated for 2 days at 37°C in DMEM containing 0.2% BSA. Cells were trypsinized, seeded into 12-well plates, and incubated for another 2 days at 37°C in DMEM plus 10% FBS. Cells were rinsed with fusion medium [10 mM Na$_2$HPO$_4$–10 mM NaH$_2$PO$_4$–150 mM NaCl–10 mM 2-(N-morpholino) ethanesulfonic acid] adjusted to pH 5.8 to 6.4 and incubated for 2 min at room temperature with pH-adjusted fusion medium. After removal of the fusion medium, cultures were replenished with DMEM containing 0.2% BSA and incubated for 1 h at 37°C. Cells were fixed with 80% ice-cold acetone and stained with Giemsa stain following the manufacturer's protocol (Fluka Chemie GmbH, Buchs, Switzerland). To quantitate fusion activities, the ratio of fused to unfused cells at a given pH was calculated in six fields for each of the variants as described previously (10).

Assay for recombinant virus pathogenicity in mice. Five 10-fold serial virus dilutions were used to infect groups of 10 6- to 8-week-old female Swiss Webster mice (Taconic, Inc.) i.c. The infection was performed under anesthesia with 10 μl of PBS containing the different virus concentrations. After infection, mice were examined for clinical signs of disease and body weight was recorded daily. The differences in body weight between day 0 and selected time points within one group were calculated, checked for the normality, and one-way analysis of variance (ANOVA) with Tukey's multiple comparisons test was applied to verify statistically significant differences between groups. The relationship between virus challenge dose and mortality was calculated using CurveExpert v.1.37 (Microsoft, Redmond, WA). All animal experiments were performed under Institutional Animal Care and Use Committee-approved protocols (Animal Welfare Assurance no A3085-01).

Immunohistochemical analysis. At different times after infection, mice were anesthetized and perfused transcardially with PBS containing procaine-HCl (5 g/liter) and heparin (20,000 IU/liter), followed by Bouin-Hollande fixation solution (11). Brains were removed and postfixed for 24 h in the same fixative. After dehydration in a graded series of 2-propanol, tissues were embedded in Paraplast Plus (Merck, Darmstadt, Germany) and cut into 7-mm-thick coronal sections. Coronal sections through the hippocampus were used for histological analysis. For enzymatic immunohistochemical analysis, adjacent sections were incubated with polyclonal rabbit antibody raised against rabies virus ribonucleoprotein (RNP) (diluted 1:3,000) (8). Primary antibodies were applied in 1% BSA-PBS and incubated at 16°C overnight, followed by a 2-h incubation at 37°C. For bright-field immunohistochemistry, species-specific biotinylated secondary antibodies (Dianova, Hamburg, Germany) and the Vectastain ABC method (Vectastain Elite ABC kit; Vector Laboratories, Burlingame, CA) were used, including ammonium nickel sulfate-enhanced 3′3-diaminobenzidine (Sigma, Deisenhofen, Germany). Immunostaining for bright-field microscopy and Giemsa stainings were analyzed with the Olympus AX70 microscope (Olympus Optical, Hamburg, Germany).

Statistical analysis. Virus spread, virus internalization, and fusion activity data were calculated and checked for normality, and a one-way ANOVA with Tukey's multiple comparisons test was applied to verify statistically significant differences between the different viruses.

RESULTS

Replacement of amino acid residue 194 of the G protein. We previously showed that the nonpathogenic phenotype of the attenuated RV strain SPBNGA is unstable (7). After five pas-

A

Asn$_{194}$ [N] → Lys$_{194}$ [K] ✳

AAT   AAG

Asn$_{194}$ [N] → Ser$_{194}$ [S] ◆

AAT   TCC

B

pSPBNGA 3'– N P M GA L –5'

pSPBNGA-K 3'– N P M GA-K ✳ L –5'

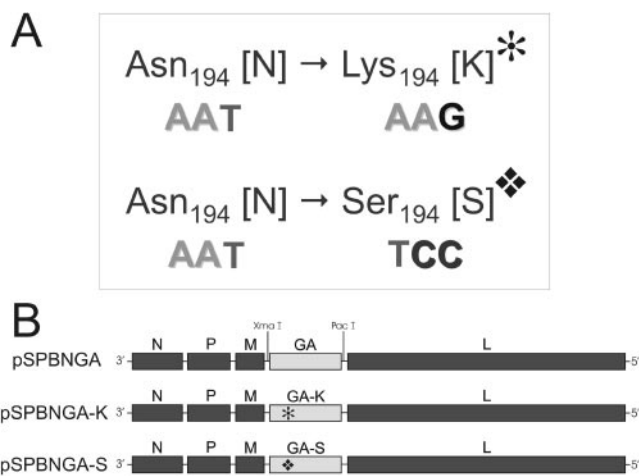pSPBNGA-S 3'– N P M GA-S ◆ L –5'

FIG. 1. Schematic of the site-directed mutagenesis of the nucleotides encoding the amino acid at position 194 of GA (A) and the construction of recombinant RVs containing the modified GA genes (B).

sages in suckling mice, an Asn→Lys mutation occurred at amino acid position 194 of GA, which was associated with increased pathogenicity in adult mice (7). To test whether the Asn$_{194}$→Lys$_{194}$ mutation alone was responsible for the increased pathogenicity, we introduced this exchange in SPBNGA using site-directed mutagenesis. In an effort to stabilize the nonpathogenic phenotype by preventing the Asn$_{194}$→Lys$_{194}$ mutation, Asn$_{194}$ was exchanged with Ser$_{194}$; reversion to the pathogenic phenotype would require three base exchanges instead of one (Fig. 1A). The mutagenized GA genes were reintroduced into the RV vector SPBNGA, resulting in SPBNGA-K with Lys at position 194 of GA and SPBNGA-S with Ser at this position (Fig. 1B).

Pathogenicity of mutant RVs in mice. The effects of SPBNGA-K and SPBNGA-S were tested in vivo, since despite complete sequencing of the G protein of the isolated pathogenic RV mutants, additional mutations in other viral genes and/or regulatory genomic elements could not be excluded.

Swiss-Webster mice infected i.c. with different concentrations (10^2 to 10^6 FFU) of SPBNGA-K showed signs of neurological disease and exhibited significant loss of body weight ($P < 0.001$), and on average 45% of these mice succumbed to the infection (Table 1; Fig. 2). Interestingly, only 10% of the

mice infected with 10^6 FFU of SPBNGA-K died, compared to 80% of mice that received 10^2 FFU of SPBNGA-K, suggesting that the mortality rate for SPBNGA-K-infected mice correlates inversely with the virus dose used for infection (correlation coefficient = 0.862 for the nonlinear Harris model). SPBNGA-K-infected mice that survived the infection exhibited neurological signs, such as disordered movement and hyperexcitation, during the entire observation period (Fig. 2B) and regained their original body weight very late (~20 days after infection) (Fig. 2C).

In contrast, regardless of the virus concentration used for infection, all mice infected i.c. with SPBNGA-S survived the infection and showed no signs of disease and only minimal loss of body weight (Fig. 2; Table 1). These data support the conclusion that an Asn$_{194}$→Lys$_{194}$ mutation in the G protein of SPBNGA is solely responsible for the increased pathogenicity observed after five mouse passages. Note that the Asn$_{194}$→Ser$_{194}$ exchange did not result in an increase in pathogenicity, indicating that Ser can functionally replace Asn at this position while conserving the SPBNGA phenotype.

To test whether the three-nucleotide exchange might increase the genetic stability of SPBNGA-S, this recombinant RV was passaged i.c. five consecutive times in newborn mice. Nucleotide sequence analysis of RV RNA isolated from brain tissue of fifth-passage mice revealed no mutations or deletions within the GA gene, and both the codon for Ser$_{194}$ and that for Glu$_{333}$ remained unchanged after the fifth passage (data not shown). Adult immunocompetent mice infected i.c. with SPBNGA-S from the fifth mouse passage revealed no mortality, morbidity, or loss of body weight, and all 10 mice survived, indicating that the nonpathogenic phenotype of SPBNGA-S is stable.

Spread GA mutant RVs in the central nervous system. To determine whether viral spread is a major factor for RV pathogenicity, brain tissue of mice infected i.c. with the different G mutants was examined immunohistochemically at 6 days p.i. Staining with RV RNP-specific antibody revealed a relatively large number of RV-infected neurons in the CA1 region of the hippocampus of mice infected with SPBNGA-K but only a low number of RNP-positive neurons in the same area of the brains from SPBNGA- or SPBNGA-S-inoculated mice (Fig. 3A). Furthermore, a massive neuronal infection of the hypothalamus was detected in SPBNGA-K-infected brains, whereas no RNP-positive neurons were found in the same

TABLE 1. Mortality and morbidity in adult mice infected i.c. with recombinant RVs

Virus Concn (FFU/10 µl)	Mortality[a]		Clinical score[b]		Loss of body weight[c]	
	SPBNGA-K	SPBNGA-S	SPBNGA-K	SPBNGA-S	SPBNGA-K	SPBNGA-S
10^6	1/9	0/10	1.3 ± 0.3	0	22.6% ± 3.0%	1.0% ± 4.0%
10^5	3/10	0/10	1.7 ± 0.6	0	24.2% ± 1.6%	0.5% ± 2.5%
10^4	6/10	0/10	2.6 ± 0.3	0	30.9% ± 2.6%	8.3% ± 3.2%
10^3	4/10	0/19	2.2 ± 0.3	0	26.1% ± 2.4%	1.4% ± 1.9%
10^2	8/10	0/10	2.8 ± 0.4	0	24.9% ± 3.5%	3.7% ± 3.7%
Average	22/49	0/49	2.1 ± 0.2	0	25.8% ± 1.4	2.9% ± 1.5

[a] Mice were infected i.c. with different concentrations of virus (10^2 to 10^6 FFU) and observed for 24 days for signs of morbidity. Values represent no. dead/no. infected.
[b] Clinical score at day 8: 0, healthy; 1, disordered movement; 2, ruffled fur, hunched back; 3, severe trembling, convulsions; 4, moribund, dehydrated.
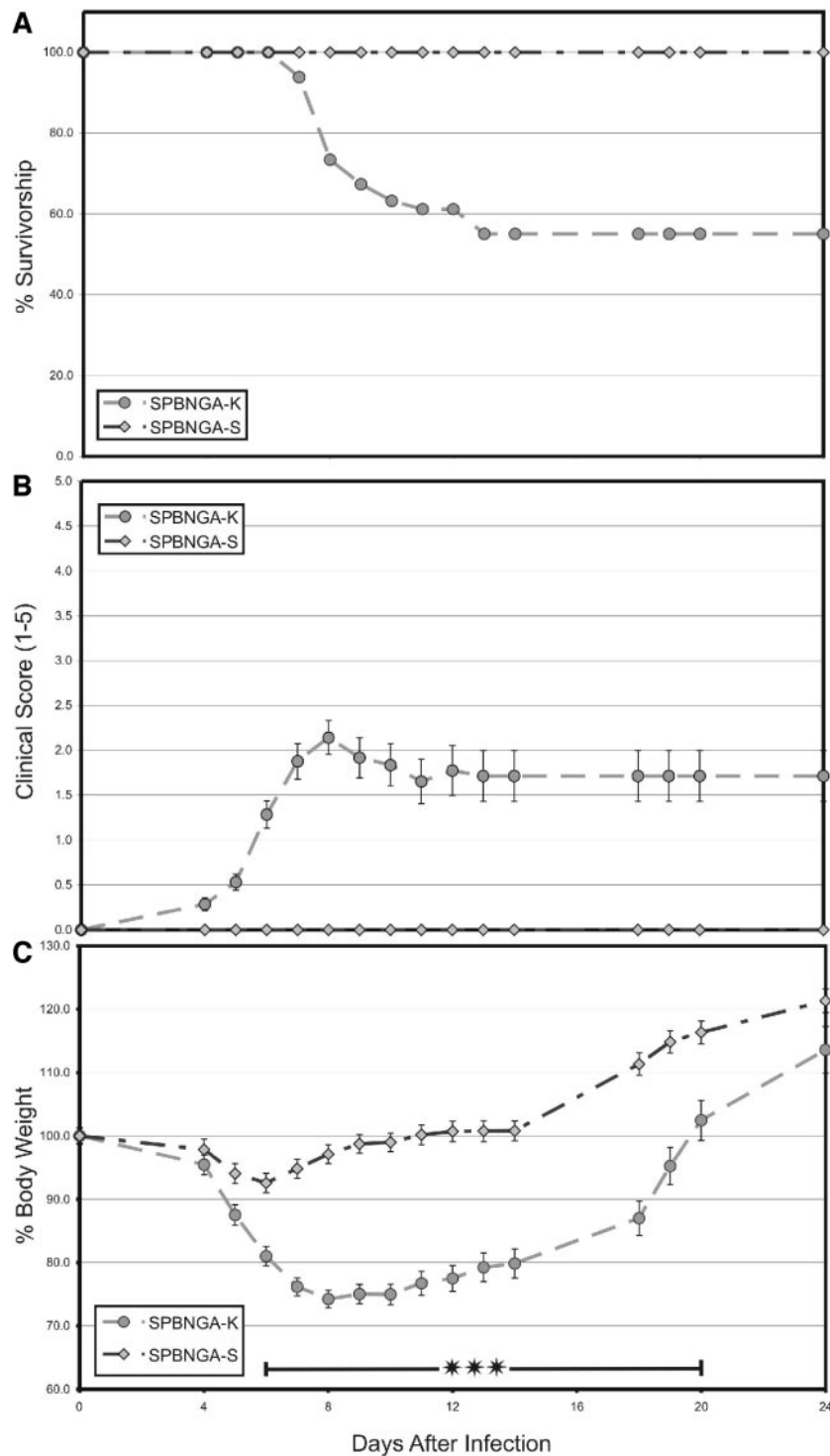[c] Loss of body weight at day 8.

FIG. 2. Mortality (A), clinical score (B), and body weight (C) of Swiss-Webster mice infected i.c. with SPBNGA-K or SPBNGA-S. Graphs represent the mean average of data obtained with the five virus concentrations listed in Table 1 (10^2 to 10^6 FFU). Error bars represent standard errors; asterisks indicate statistically significant differences in the decrease of body weight ($P < 0.001$) between SPBNGA-K-infected and SPBNGA-S-infected mice.

region of SPBNGA- and SPBNGA-S-infected brains (Fig. 3B). Thus, the $Asn_{194} \rightarrow Lys_{194}$ exchange but not the $Asn_{194} \rightarrow Ser_{194}$ exchange markedly increased the ability of SPBNGA to spread in brain tissue.

Growth kinetics of GA mutant RVs in neuronal cells. Virus production was analyzed in a neuroblastoma cell line (NA), and both multistep (Fig. 4A) and single-step (Fig. 4B) growth curves were constructed. Surprisingly, the replication rate of
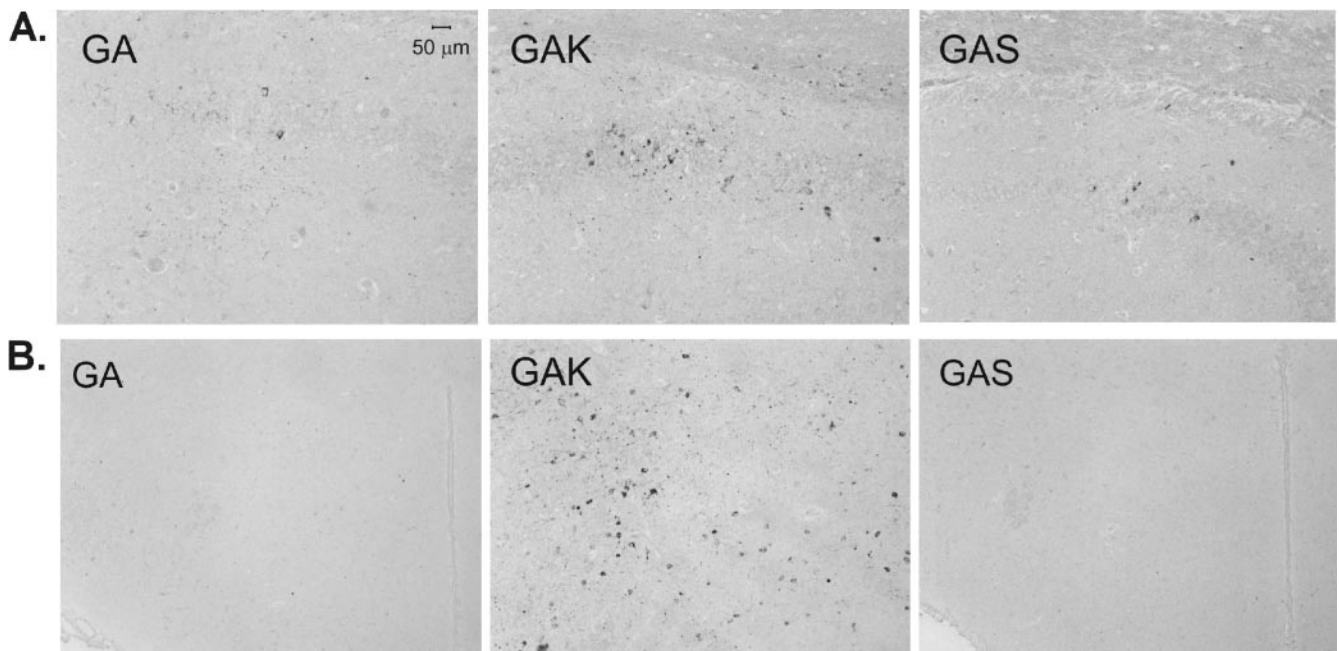
FIG. 3. Immunohistological analysis of rabies virus-infected neurons in the CA1 region of the hippocampal formation (A) and hypothalamus (B) of Swiss-Webster mice infected with SPBNGA, SPBNGA-K, or SPBNGA-S. RNP-specific antibody was used for immunostaining. Bar = 50 μm in all panels.

SPBNGA-K was significantly lower (~1 log; $P < 0.001$) than that of SPBNGA or SPBNGA-S. Thus, while the $Asn_{194} \rightarrow Ser_{194}$ exchange had no affect on virus production, the $Asn_{194} \rightarrow Lys_{194}$ mutation in SPBNGA-K decreased virus replication in tissue culture.

Kinetics of cell-to-cell spread of GA mutant viruses. Because NA cells cannot be overlaid with agar, cell-to-cell spread was analyzed in the neuronal cell line N2A after infection at a MOI of 0.01 with the different mutant viruses (Fig. 5). Evaluation by immunofluorescence microscopy revealed no significant differences in the number of fluorescent foci in SPBNGA-, SPBNGA-K-, and SPBNGA-S-infected N2A cells at 24 h p.i. with an average of 1.1, 1.3, and 1 infected cell per focus. However, at 72 h p.i., 17, 30, and 15 cells were counted on average for each fluorescent focus of SPBNGA-, SPBNGA-K- and SPBNGA-S-infected N2A cells, respectively, indicating that the rate of SPBNGA-K spread is almost twice those for SPBNGA ($P < 0.001$) and SPBNGA-S ($P < 0.001$).

Kinetics of internalization of GA mutant viruses. To determine whether the faster spread of SPBNGA-K might reflect the more rapid uptake of the virus by cells, the mutant RVs were used to infect NA cells, and at various times p.i., neutralizing polyclonal rabies antibody was added to neutralize non-internalized virus. When the antibody was added at 20 min p.i., viral antigen was detected in 60% of SPBNGA-K-infected cells but in only 25% and 31% of cells infected with SPBNGA-S or SPBNGA, respectively (Fig. 6). The time necessary to infect 50% of cells (half entry time) was 17 min for SPBNGA-K and 29.5 and 33.5 min for SPBNGA and SPBNGA-S, respectively. Thus, the $Asn_{194} \rightarrow Lys_{194}$ exchange in the G protein, the only RV component involved in virus uptake by the host cell, drastically reduces the time for virus uptake, which, in turn, might account for the increase in pathogenicity and viral spread.

pH-dependent fusion of GA mutant virus-infected cells. It has been suggested that the ability of an RV to spread from cell to cell depends on the fusion activity of its G protein (14, 19, 28). We determined the pH-dependent cell fusion in SPBNGA-K-, SPBNGA-N, and SPBNGA-S-infected BSR cells (Fig. 7). Thirty percent of SPBNGA-K-infected cells were fused at pH 6.2, compared to 23% and 12% of SPBNGA-N- and SPBNGA-S-infected cells, respectively. The greatest differences in fusion activity were observed at pH 6.0, where 86% of the SPBNGA-K-infected cells but only 63% and 46% of the SPBNGA-N- and SPBNGA-S-infected cells were fused. The differences in the fusion activities seen in SPBNGA-K- and SPBNGA-N- or SPBNGA-S-infected cells are statically significant ($p \ll 0.0001$) within the pH range from 5.8 to 6.2, indicating that the $Asn_{194} \rightarrow Lys_{194}$ mutation causes a shift in the pH threshold for membrane fusion to a slightly higher pH.

DISCUSSION

The multiple factors that influence RV pathogenicity have proven difficult to dissect experimentally when using different RV isolates (25), since numerous sequence differences between genes of different RV strains, as exemplified after the complete sequences of the pathogenic RV Pasteur virus and attenuated RV vaccine strain SAD B19 became available (3, 27), precluded linkage of a certain sequence to the observed differences in pathogenicity. However, the ability to genetically manipulate the genome of RV and to introduce specific
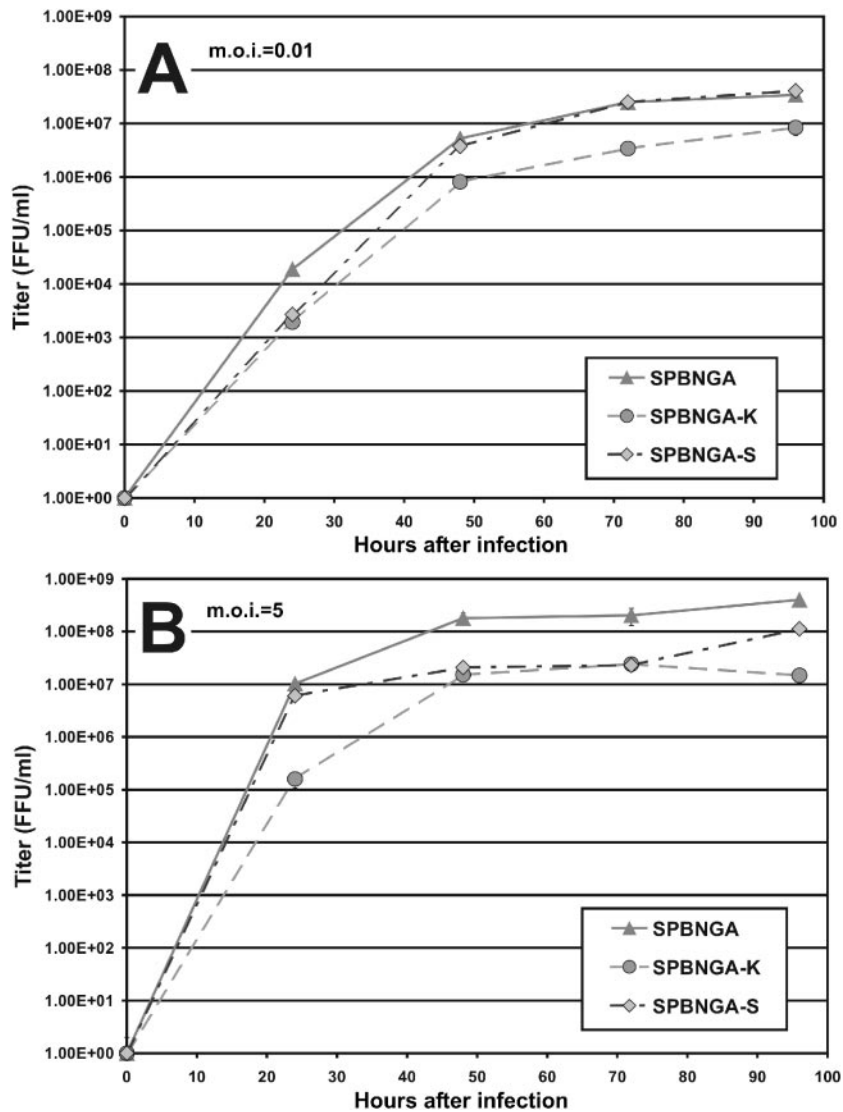
FIG. 4. Multistep (A) and single-step (B) virus growth curves of recombinant RV in NA cells. NA cells were infected with SPBNGA, SPBNGA-K, or SPBNGA-S at a MOI of 0.01 (A) or a MOI of 5 (B) and incubated at 34°C. At the indicated times after infection, viruses were harvested and titrated. Data are the means (plusmn standard error) of four virus titer determinations for NA cells.

mutations within the same RV backbone (24) has enabled us to identify several RV pathogenicity markers (9, 16, 21–22).

It has been known for more than 20 years that an amino acid exchange in certain attenuated RV strains at position 333 from Arg to Glu abolishes residual RV pathogenicity even after i.c. injection in adult mice (6). However, the genetic stability of this mutation, based on a single nucleotide exchange, raised concern about its use as a vaccine. We previously showed that multiple passages of an RV with the 333 mutation in newborn mice resulted in revertant RVs that partially recovered the pathogenic phenotype of SPBN (7). This pathogenic revertant RV contained an exchange at position 194 from Asn to Lys instead of an exchange at position 333 from Glu to Arg. By introducing the $Asn_{194} \rightarrow Lys_{194}$ mutation into SPBNGA, we were able to show that this single amino acid exchange was solely responsible for the reemergence of the pathogenic phenotype. Note that the $Asn_{194} \rightarrow Lys_{194}$ mutation is located in a

region of G that was shown to determine the pathogenic phenotype of the Nishigahara RV strain (12). Our observation that the mortality in SPBNGA-K-infected mice seemed to correlate inversely with the virus dose used for infection is probably due to autointerference. This phenomenon is not new and has been earlier described for mice infected with attenuated RV strains (2).

Our present data clearly indicate that SPBNGA-K spreads faster both in vitro, as indicated by a larger focus size in cell culture, and in vivo, as shown by immunochemistry of infected mouse brains. However, SPBNGA-K grew to lower titers in NA cells, as indicated by single-step and multiple-step growth curves. This apparent discrepancy with the data indicating an increased virus load in the brains of SPBNGA-K-infected mice likely rests in the faster spread of SPBNGA-K from neuron to neuron, resulting in a higher number of infected neurons in vivo. This conclusion is consistent with previous studies showing that pathogenic RVs replicate in vitro at a slower rate and
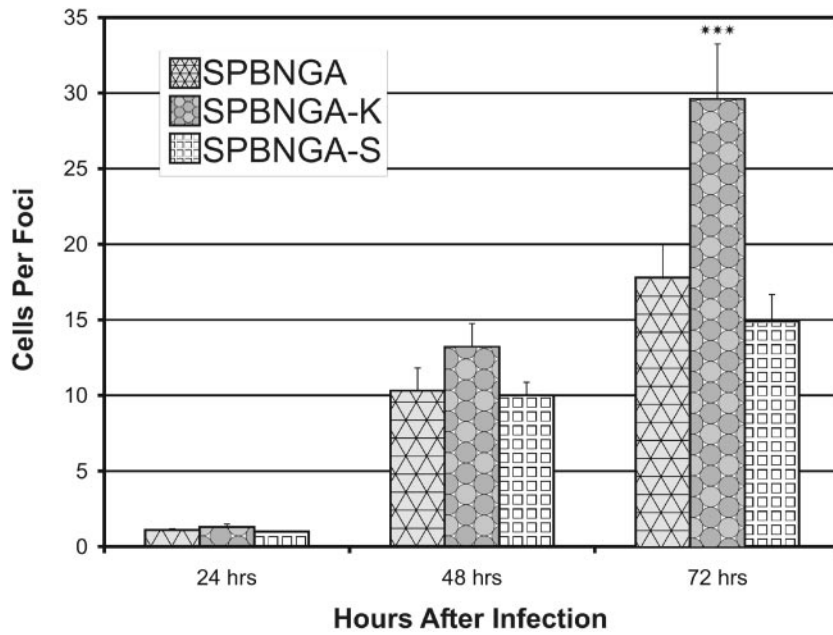
FIG. 5. Cell-to-cell spread of SPBNGA, SPBNGA-K, or SPBNGA-S in N2A cells. Cells were infected at a MOI of 0.01, overlaid with 1% agar, incubated at 34°C for the indicated times, fixed with acetone, and stained with FITC-labeled rabies virus N protein-specific antibody. Thirty fluorescent foci were examined to determine the number of infected cells per fluorescent focus. Error bars represent standard errors; asterisks indicate statistically significant differences (∗∗∗, $P < 0.001$) between two experimental groups.

produce lesser amounts of viral proteins but spread faster than attenuated RV strains (for a review, see references 4 and 25).

The finding that SPBNGA-K enters cells at twice the rate of SPBNGA or SPBNGA-S entry suggests that faster virus uptake underlies at least in part the increase in cell-to-cell spread and consequently the greater pathogenicity of SPBNGA-K.

This suggestion is supported by the recent observations that the highly pathogenic SHBRV strain is internalized four times faster than the attenuated SPBN strain (9).

We also detected a small but significant change in the pH required for membrane fusion of the SPBNGA-K G protein. Other studies have demonstrated the importance of the pH-
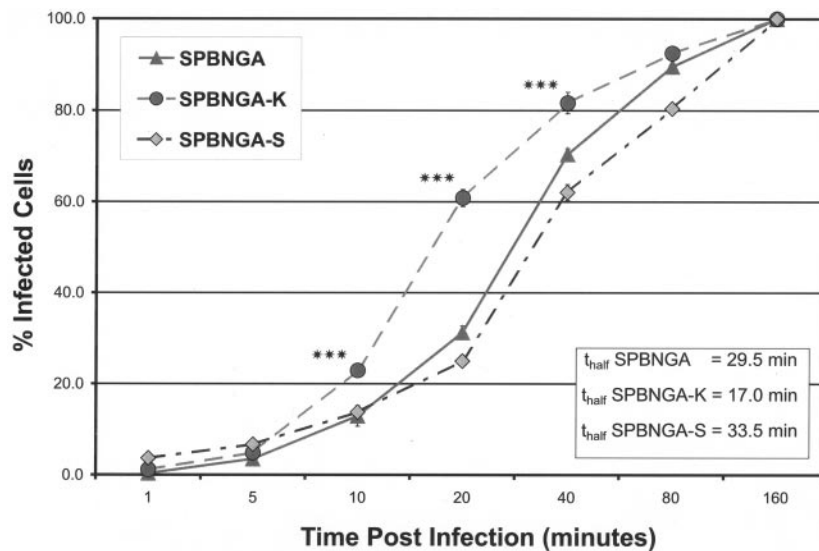

FIG. 6. Effect of mutations of amino acid 194 in RV GA protein on the kinetics of virus internalization. Monolayers of NA cells grown in 96-well plates were infected with SPBNGA, SPBNGA-K, or SPBNGA-S at a multiplicity of infection of 5. Neutralizing polyclonal antibody was added at the indicated times p.i. to neutralize noninternalized RV. At 20 h p.i., cells were examined for the presence of RV antigen by the fluorescent-antibody technique, and the percentage of infected cells was determined. Each value represents the mean (± standard error of the mean) from 12 individual wells. Asterisks indicate statistically significant differences (∗∗∗, $P < 0.001$) between two experimental groups. T_{half}, time needed to infect 50% of cells.
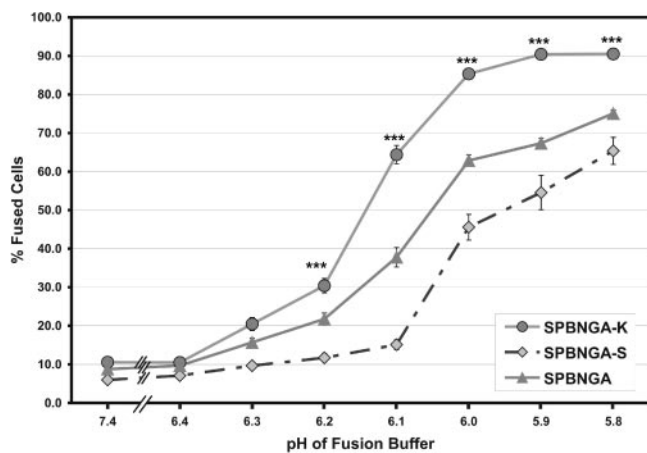
FIG. 7. pH dependence of cell fusion. BSR cells infected with recombinant RVs were treated with fusion medium at the indicated pH and incubated for 1 h at 37°C. The percentage of fused cells was determined as described in Materials and Methods. Error bars represent standard errors, and asterisks indicate statistically significant differences (∗∗∗, $P < 0.001$).

dependent fusion process for the initiation of productive infection by vesicular stomatitis virus, another rhabdovirus whose G protein mediates the fusion (14, 19, 28). Attenuation of vesicular stomatitis virus variants for growth in tissue culture has been attributed to a shift in the pH for membrane fusion to a lower pH (10). Our studies are consistent with this finding and, together with the association between an $Asn_{194} \rightarrow Lys_{194}$ exchange in the G protein of RV and a significant increase in virus spread in vitro and in vivo, support the hypothesis that a higher pH threshold for membrane fusion is important for viral fitness (10).

In summary, our study provides evidence that a single amino acid exchange within the G protein of a nonpathogenic RV can result in a reversion to the pathogenic phenotype. The increase in pathogenicity is due to a significant increase in viral spread both in vitro and in vivo. Our results also indicate that the generation of a revertant RV carrying this exchange can be prevented by introducing a Ser instead of the Asn at position 194. The SPBNGA-S strain remained stable even after multiple passages in newborn mice, making its glycoprotein suitable for the generation of both wildlife RV vaccines and RV-based vaccine vectors (7–8, 16–18, 22).

REFERENCES

1. **Centers for Disease Control and Prevention.** 1999. Human rabies prevention. Morb. Mortal. Wkly. Rep. **48:**1–21.
2. **Clark, H. F.** 1980. Rabies serogroup viruses in neuroblastoma cells: propagation, "autointerference," and apparently random back-mutation of attenuated viruses to the virulent state. Infect. Immun. **27:**1012–1022.
3. **Conzelmann, K. K., J. H. Cox, L. G. Schneider, and H. J. Thiel.** 1990. Molecular cloning and complete nucleotide sequence of the attenuated rabies virus SAD B19. Virology **175:**485–499.
4. **Dietzschold, B., M. Faber, and M. J. Schnell.** 2003. New approaches to the prevention and eradication of rabies. Expert Rev. Vaccines **2:**89–96.
5. **Dietzschold, B., T. J. Wiktor, J. Q. Trojanowski, R. I. MacFarlan, W. H. Wunner, M. J. Torres-Anjel, and H. Koprowski.** 1985. Differences in cell-to-cell spread of pathogenic and apathogenic rabies virus in vivo and in vitro. J. Virol. **56:**12–18.
6. **Dietzschold, B., W. H. Wunner, T. J. Wiktor, A. D. Lopes, M. Lafon, C. L. Smith, and H. Koprowski.** 1983. Characterization of an antigenic determinant of the glycoprotein that correlates with pathogenicity of rabies virus. Proc. Natl. Acad. Sci. USA **80:**70–74.
7. **Dietzschold, M. L., M. Faber, J. A. Mattis, K. Y. Pak, M. J. Schnell, and B. Dietzschold.** 2004. In vitro growth and stability of recombinant rabies viruses designed for vaccination of wildlife. Vaccine **23:**518–524.
8. **Faber, M., R. Pulmanausahakul, S. S. Hodawadekar, S. Spitsin, J. P. McGettigan, M. J. Schnell, and B. Dietzschold.** 2002. Overexpression of the rabies virus glycoprotein results in enhancement of apoptosis and antiviral immune response. J. Virol. **76:**3374–3381.
9. **Faber, M., R. Pulmanausahakul, K. Nagao, M. Prosniak, A. B. Rice, H. Koprowski, M. J. Schnell, and B. Dietzschold.** 2004. Identification of viral genomic elements responsible for rabies virus neuroinvasiveness. Proc. Natl. Acad. Sci. USA **101:**16328–16332.
10. **Fredericksen, B. L., and M. A. Whitt.** 1995. Vesicular stomatitis virus glycoprotein mutations that affect membrane fusion activity and abolish virus infectivity. J. Virol. **69:**1435–1443.
11. **Hooper, D. C., K. Morimoto, M. Bette, E. Weihe, H. Koprowski, and B. Dietzschold.** 1998. Collaboration of antibody and inflammation in clearance of rabies virus from the central nervous system. J. Virol. **72:**3711–3719.
12. **Ito, N., M. Takayama, K. Yamada, M. Sugiyama, and N. Minamoto.** 2001. Rescue of rabies virus from cloned cDNA and identification of the pathogenicity-related gene: glycoprotein gene is associated with virulence for adult mice. J. Virol. **75:**9121–9128.
13. **Lentz, T. L., T. G. Burrage, A. L. Smith, J. Crick, and G. H. Tignor.** 1982. Is the acetylcholine receptor a rabies virus receptor? Science **215:**182–184.
14. **Mannen, K., M. Ohuchi, and K. Mifune.** 1982. pH-dependent hemolysis and cell fusion of rhabdoviruses. Microbiol. Immunol. **26:**1035–1043.
15. **Martinez, L.** 2000. Global infectious disease surveillance. Int. J. Infect. Dis. **4:**222–228.
16. **McGettigan, J. P., R. J. Pomerantz, C. Siler, P. M. McKenna, H. D. Foley, B. Dietzschold, and M. J. Schnell.** 2003. Second generation rabies-based vaccine vectors expressing HIV-1 Gag have greatly reduced pathogenicity but are highly immunogenic. J. Virol. **77:**237–244.
17. **Mebatsion, T.** 2001. Extensive attenuation of rabies virus by simultaneously modifying the dynein light chain binding site in the P protein and replacing Arg333 in the G protein. J. Virol. **75:**11496–11502.
18. **Mebatsion, T., F. Weiland, and K. K. Conzelmann.** 1999. Matrix protein of rabies virus is responsible for the assembly and budding of bullet-shaped particles and interacts with the transmembrane spike glycoprotein G. J. Virol. **73:**242–250.
19. **Mifune, K., M. Ohuchi, and K. Mannen.** 1982. Hemolysis and cell fusion by rhabdoviruses. FEBS Lett. **137:**293–297.
20. **Morimoto, K., D. C. Hooper, S. Spitsin, H. Koprowski, and B. Dietzschold.** 1999. Pathogenicity of different rabies virus variants inversely correlates with apoptosis and rabies virus glycoprotein expression in infected primary neuron cultures. J. Virol. **73:**510–518.
21. **Morimoto, K., H. D. Foley, J. P. McGettigan, M. J. Schnell, and B. Dietzschold.** 2000. Reinvestigation of the role of the rabies virus glycoprotein in viral pathogenesis using a reverse genetics approach. J. Neurovirol. **6:**373–381.
22. **Morimoto, K., J. P. McGettigan, H. D. Foley, D. C. Hooper, B. Dietzschold, and M. J. Schnell.** 2001. Genetic engineering of live rabies vaccines. Vaccine **19:**3543–3551.
23. **Rupprecht, C. E., J. S. Smith, M. Fekadu, and J. E. Childs.** 1995. The ascension of wildlife rabies: a cause for public health concern or intervention? Emerg. Infect. Dis. **1:**107–114.
24. **Schnell, M. J., T. Mebatsion, and K. K. Conzelmann.** 1994. Infectious rabies viruses from cloned cDNA. EMBO J. **13:**4195–4203.
25. **Schnell, M. J., G. S. Tan, and B. Dietzschold.** 2005. The application of reverse genetics technology in the study of rabies virus (RV) pathogenesis and for the development of novel RV vaccines. J. Neurovirol. **11:**76–81.
26. **Seif, I., P. Coulon, P. E. Rollin, and A. Flamand.** 1985. Rabies virulence: effect on pathogenicity and sequence characterization of rabies virus mutations affecting antigenic site II of the glycoprotein. J. Virol. **53:**926–934.
27. **Tordo, N., O. Poch, A. Ermine, G. Keith, and F. Rougeon.** 1986. Walking along the rabies genome: is the large G-L intergenic region a remnant gene? Proc. Natl. Acad. Sci. USA **83:**3914–3918.
28. **Whitt, M. A., L. Buonocore, C. Prehaud, and J. K. Rose.** 1991. Membrane fusion activity, oligomerization, and assembly of the rabies virus glycoprotein. Virology **185:**681–688.
29. **Winkler, W. G., and K. Bogel.** 1992. Control of rabies in wildlife. Sci. Am. **266:**86–92.